

A new method for analyzing second-order phase transitions applied to the ferromagnetic transition of a polaronic system

J. A. Souza^{1,2}, Yi-Kuo Yu³, J. J. Neumeier¹, H. Terashita¹ and R. F. Jardim²

¹*Department of Physics, P. O. Box 173840, Montana State University, Bozeman, MT 59717-3840*

²*Instituto de Física, Universidade de São Paulo, CP 66318, 05315-970, São Paulo, Brazil and*

³*National Center for Biotechnology Information, NIH, 8600 Rockville Pike, Bethesda, MD 20894*

(Dated: January 18, 2022)

A new method for analyzing second-order phase transitions is presented and applied to the polaronic system $\text{La}_{0.7}\text{Ca}_{0.3}\text{MnO}_3$. It utilizes heat capacity and thermal expansion data simultaneously to correctly predict the critical temperature's pressure dependence. Analysis of the critical phenomena reveals second-order behavior and an unusually large heat capacity exponent.

PACS numbers: 75.40.Cx, 65.20.+w, 75.47.Lx, 75.30.Kz

Investigations of phase transitions are important for our fundamental understanding of condensed matter systems and of wider interest because these systems can serve as environments for the study of topological defects [1]. The phase transition in manganese oxides exhibiting colossal magnetoresistance (CMR) is particularly fascinating since competition among the charge, lattice, and spin degrees of freedom leads to the CMR effect [2]. Double-exchange interactions among the magnetic ions and electron-phonon coupling via the Jahn-Teller distortion play essential roles, especially near the ferromagnetic (FM) to paramagnetic (PM) phase transition where the metal-insulator transition occurs and the CMR effect is the largest. Defects known as magnetic polarons form well above the critical temperature T_c and increase in density as the temperature is lowered through T_c [2, 3]. The complexity of this phase transition has led to uncertainty as to its thermodynamic characterization [4].

The first-order phase transition line, along which two thermodynamic phases coexist on a phase diagram, is described by the Clausius-Clapeyron equation. Across this line the first derivative of the free energy is discontinuous. This results in the divergence at T_c of quantities, such as the molar heat capacity at constant pressure C_P or the thermal expansion coefficient μ , but no sign of divergence occurs prior to approaching T_c . In general, this generic feature is not compromised by finite system size because the correlation length remains finite at T_c and is typically much smaller than the sample size. In contrast, the second-order (continuous) phase transition occurs with diverging correlation length as T_c is approached, indicating a scale-free phenomena. It is possible to generalize from first-order transitions with discontinuous first derivatives of the free energy to n th-order transitions with discontinuous n th-derivatives [5]. Indeed, the Ehrenfest equation

$$\frac{dT_c}{dP} = \frac{vT_c\Delta\Omega}{\Delta C_P}, \quad (1)$$

is a generalization of the Clausius-Clapeyron equation to second-order transitions (v is the molar volume, ΔC_P

and $\Delta\Omega = 3\Delta\mu$ are the jumps in C_P and the volume thermal expansion coefficient Ω at T_c , and P is the pressure). Interestingly, the only phase transition known to exhibit distinct jumps in C_P and Ω and obey Eq. (1) is the normal-superconductor transition [6]. For most systems undergoing continuous phase transitions, instead of jumps in C_P and Ω , critical behavior is observed. More specifically, near T_c , C_P (with $t \equiv (T - T_c)/T_c$) is dominated by $C_P \sim |t|^{-\alpha_{\pm}}$. The exponents α_{\pm} are called the critical exponents above (+) and below (−) T_c . Apparently, if C_P or Ω exhibit critical behavior, the quantities ΔC_P and $\Delta\Omega$ in Eq. (1) are not well defined. One result of this letter is a substitute for Eq. (1), that is widely applicable for calculating dT_c/dP using C_p and Ω data.

With T and P as independent variables, the thermodynamic potential per mole $\Phi = u - TS + Pv$ is used to derive the needed thermodynamic equality (u and S are the internal energy and entropy per mole). Let $T_c(P)$ be the critical temperature at pressure P ; it marks a phase transition line on the (T, P) plane. We assume, within the pressure range of interest, that $T_c(P)$ can be inverted into $P(T_c)$. The molar entropy at $T_c(P)$, $S(T_c, P(T_c))$, abbreviated by $S(T_c)$, marks a transition line on the (T, S) plane as well. Given a small temperature shift δ away from a fixed T_c and starting at $(T_c + \delta, P(T_c))$ on the (T, P) plane, we move an infinitesimal amount parallel to the transition line $P(T_c)$. It is easy to show that such movement also moves the point $(T_c + \delta, S(T_c))$ on the (T, S) plane parallel to the line $S(T_c)$. The displacements dS , dT , and dP are related through

$$TdS = C_P dT - vT\Omega dP. \quad (2)$$

This immediately leads to

$$C_P = T \left(\frac{\partial S}{\partial T} \right)_c + vT\Omega \left(\frac{\partial P}{\partial T} \right)_c, \quad (3)$$

which holds for $T \equiv T_c + \delta$ above and below T_c ; $(\partial S/\partial T)_c$ and $(\partial P/\partial T)_c$ are slopes of the phase transition lines at fixed T_c on the (T, S) and (T, P) planes, respectively. Eq. (3) implies that, near T_c , one can superimpose $C_p^* \equiv$

$C_p - a - bT$ with [7] $T\Omega$ after rescaling of $T\Omega$; v is treated as a constant since it changes only slightly, $< 0.1\%$, near T_c . This relation also indicates that if C_p diverges, $T\Omega$ diverges with the same exponent.

We investigate a CMR oxide for which it has been difficult to determine whether the phase transition is first or second order [4, 8, 9, 10, 11, 12]. Polycrystalline $\text{La}_{0.7}\text{Ca}_{0.3}\text{MnO}_3$ was prepared by mixing stoichiometric amounts of $\text{La}(\text{NO}_3)_3 \cdot 6\text{H}_2\text{O}$, $\text{Ca}(\text{NO}_3)_2 \cdot 4\text{H}_2\text{O}$, and $\text{C}_4\text{H}_6\text{MnO}_4 \cdot 4\text{H}_2\text{O}$ in distilled water and a 50 mol% excess of citric acid and ethylene glycol. The solution was heated at 120°C , stirred until a gel formed and then dried. The organic material was oxidized 24 h at 500°C . The powder was ground with an agate mortar for 30 min, heat treated 30 h at 1000°C , ground for 30 min, and heat treated 30 h at 1100°C . Finally, the powder was ground for 30 min, pressed into pellets and reacted 30 h at 1200°C . The density was $5.47(2) \text{ gm/cm}^3$ (90% of theoretical density) and x-ray powder diffraction confirmed the single-phase nature. Four-probe electrical resistivity and ac susceptibility (500 Hz) were measured under hydrostatic pressure in a Fluorinert medium; a manganin sensor determined pressure at 295 K. A fused quartz capacitive dilatometer was used to observe the linear thermal expansion with a sensitivity in Δl of 0.1 \AA ; for the 2.6 mm long sample, the relative sensitivity is about four orders of magnitude better than diffraction methods. Heat capacity and dc magnetization were measured with a Quantum Design PPMS. All data were obtained on the same sample.

C_p and S ($S(T) = \int (C_p/T) dT$) are shown in Fig. 1(a). The anomaly in C_p is associated with the *PM* to *FM* transition. To obtain S associated with the magnetic transition, S_{MAG} , a polynomial fit from 80 K to 325 K (excluding the region $200 \text{ K} \leq T \leq 270 \text{ K}$) was subtracted; S_{MAG} (upper inset of Fig. 1(a)) reveals a smooth change at T_c . The entropy value 3.2 J/mol.K at $T = 300 \text{ K}$, agrees with prior reports [12, 13]. The thermal expansion coefficient $\mu(T)$ is illustrated in Fig. 1(b); μ was determined by taking a point-by-point derivative of $\Delta l/l_0$ (shown near T_c in the inset), it reveals an anomaly at T_c as well. Straight lines are drawn through C_p and μ above and below T_c illustrating the form of an ideal second-order phase transition [5]. This provides $\Delta C_p = -7.45(5) \text{ J/mol.K}$ and $\Delta\Omega = 3\Delta\mu = -9.60(12) \times 10^{-6} \text{ K}^{-1}$. Eq. (1) is applied to estimate the pressure derivative $dT_c/dP = 11.5(2) \text{ K/GPa}$ using $T_c = 249.5 \text{ K}$ and $v = 3.57 \times 10^{-5} \text{ m}^3/\text{mol}$. Magnetic susceptibility at 2000 Oe, $\mu(T)$ and $C_p(T)$ all reveal $T_c = 249.5 \text{ K}$.

To apply Eq. (3), the overlap between C_p^* [7] and $\lambda\mu T$ is maximized with $a = 59.5 \text{ J/mol.K}$, $b = 0.128 \text{ J/mol.K}^2$ and $\lambda = 7000 \pm 300 \text{ J/mol.K}$. The proportionality between C_p^* and μT (Fig. 2) suggests: (1) S must be continuous and differentiable along (and in the vicinity of) the phase transition line and (2) v at a given pressure is continuous across T_c ; therefore, the phase transition is continuous (second order). Furthermore, the quantity

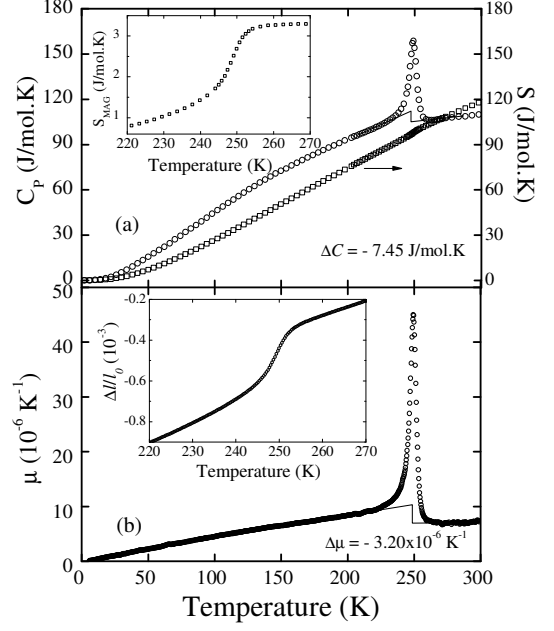


FIG. 1: (a) Molar heat capacity C_p , molar entropy S , and magnetic entropy S_{MAG} (inset) versus T . (b) Expansion coefficient μ and $\Delta l/l_0$ (inset); l_0 is the length at 300 K. Lines denote the jumps for an ideal second-order phase transition.

dT_c/dP is now given by

$$\frac{dT_c}{dP} \equiv \left(\frac{\partial P}{\partial T} \right)_c^{-1} = \frac{3v\mu T}{C_p^*} = 15.3(7) \text{ K/GPa}. \quad (4)$$

In Fig. 2, C_p^* displays more rounding of the peak than μ ; this is associated with the heat pulse which changes the sample temperature by ΔT ($\sim 2.5 \text{ K}$ near T_c) at each measurement temperature. This leads to an averaging effect [14] that is absent in the thermal expansion data which is acquired closer to equilibrium (warming rates $< 8 \text{ K/h}$). In addition, there is a smaller effective sample size in the C_p data because the heat pulse cannot warm the sample uniformly and simultaneously.

Before comparing dT_c/dP in Eq. (4) with experiment, critical exponents are determined. This usually requires a background subtraction to enlarge the range of validity of power-law behavior. Although more complicated background subtractions might, in general, be necessary, we allow only two constant shifts A_{\pm} in the expression of μT . That is, we assume that when $T > T_c$ ($T < T_c$), μT can be fitted by the expression $A_{+(-)} + (B_{+(-)}/\alpha)|t|^{-\alpha}$. Making a grid for $-12 \leq A_{\pm} \leq 12$ and $248 \text{ K} \leq T_c \leq 251 \text{ K}$ and plotting $|t|$ versus $7000\mu T - A_{\pm}$ on a log-log scale, we choose the set of A_{\pm} and T_c that maximize the power-law fittable temperature range and minimize the deviation within the fitted range ($220 \text{ K} < T < 270 \text{ K}$). Using the optimal A_{\pm} and T_c , $C_p^* - A_{\pm}$ and $7000\mu T - A_{\pm}$ versus t are plotted in Fig. 3. The ability to obtain a power-law fit above and below T_c with the same exponent agrees

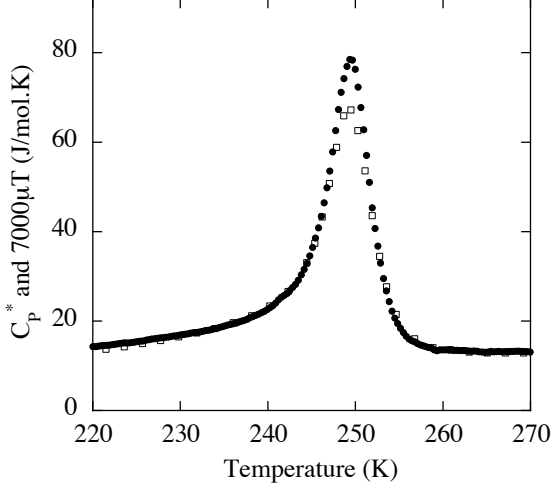


FIG. 2: Molar heat capacity after subtracting a linear term, C_P^* (open symbols), and $7000\mu T$ (closed symbols) versus T illustrating the scaling suggested by Eq. (3).

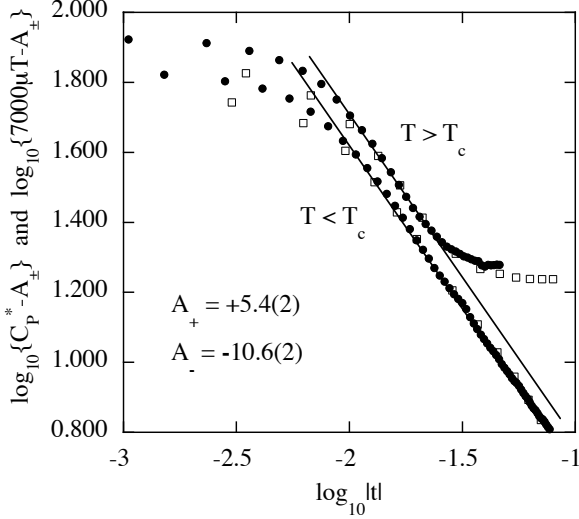


FIG. 3: $C_P^* - A_{\pm}$ (open symbols) and $7000\mu T - A_{\pm}$ (closed symbols) versus $t \equiv (T - T_c)/T_c$ on a log-log scale.

well with the one-parameter scaling theory of continuous phase transitions. The smaller reduced temperature range for $T > T_c$ indicates that the fluctuation-induced ordered domains grow to macroscopic size only when T is close to T_c . This implies that the prefactor for the correlation length $\xi \sim g_{\pm}|t|^{-\nu}$ is smaller on the high temperature side ($g_+ < g_-$). The exponent $\alpha_{\pm} = 0.93(8)$ is obtained whose magnitude is significant since $\alpha_{\pm} \geq 1$ would lead to a divergence in the integrals of C_P and μ near T_c [17]. This explains why this continuous (second-order) phase transition, evidenced by the superposition of C_P^* and $7000\mu T$, has often been characterized as first order or nearly first order. The same measurements and analysis on a second sample of $\text{La}_{0.7}\text{Ca}_{0.3}\text{MnO}_3$ yielded identical results for α_{\pm} [18].

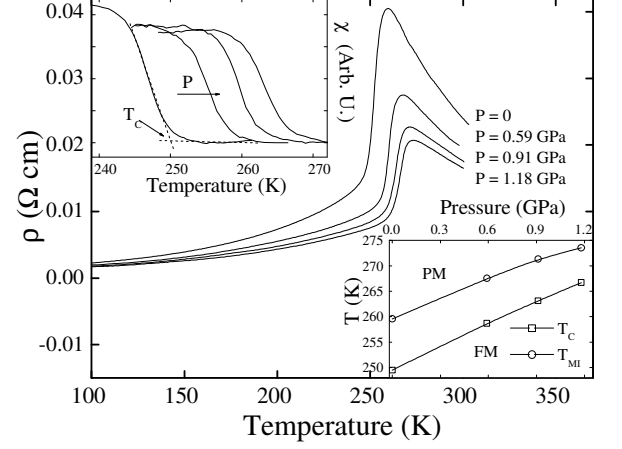


FIG. 4: Electrical resistivity and ac susceptibility (upper inset) versus T under pressure P . Lines illustrate T_c determination. Lower inset shows T_c and T_{MI} versus P .

To test Eqs. (1) and (4), dT_c/dP was measured. Fig. 4 shows the electrical resistivity $\rho(T, P)$. Pressure decreases ρ and shifts the metal-insulator transition temperature T_{MI} upward. In the left inset of Fig. 4, the pick-up coil signal is shown and lines illustrate the manner in which T_c was determined. The (T, P) phase diagram is shown in the lower inset. These results reveal that $dT_{MI}/dP \cong dT_c/dP = 16.5(3)$ K/GPa [15], which is 43% larger than the value of $11.5(2)$ K/GPa calculated by Eq. (1), but in better agreement with $15.3(7)$ K/GPa calculated by Eq. (4). The wide range of dT_c/dP values (12 to 22 K/GPa) [9, 16] for this composition ($x = 0.30$ and 0.33 values are noted here) illustrates that all quantities appearing in Eqs. (1) and (4) must be determined on the same specimen in order to conduct a meaningful analysis.

As noted above, agreement has not been reached regarding how to characterize the phase transition of $\text{La}_{0.7}\text{Ca}_{0.3}\text{MnO}_3$ (and compositions close to this). Heat capacity measurements on $\text{La}_{0.67}\text{Ca}_{0.33}\text{MnO}_3$ were unable to determine the critical exponent indicating that the phase transition was first order; however, critical exponents for $\text{La}_{0.6}\text{Ca}_{0.4}\text{MnO}_3$ were obtained, which led to the assertion that it defines a tricritical point in the phase diagram [12]. Our results together with those of Kim et al. [12], indicate that further investigations are needed to determine the compositional dependence of α_{\pm} . An analysis [11] ($\text{La}_{0.65}\text{Ca}_{0.35}\text{MnO}_3$) using the Clausius-Claperyon equation suggested that the phase transition was first order. We have also applied this method and found dT_c/dP in agreement with our measurements; however, this is fortuitous since the Clausius-Claperyon equation is valid for transitions where S and v make *discontinuous* changes at T_c , which is clearly not the case (see insets of Fig. 1). In comparing our study

to others, it is essential to consider: (1) the scaling between C_p^* and μT , (2) the use of *both* in obtaining the critical exponent and (3) α_{\pm} is close to 1 resulting in *near-divergences* of C_p and μ which clarifies why the transition has often been identified as first order.

Establishing the continuous (second-order) nature of the phase transition has important implications. Above T_c , magnetic defects (polarons) form which grow in density as the sample is cooled through T_c [2, 3]. Our results suggest a divergent magnetic correlation length at T_c *only* if the magnetization is the correct order parameter in CMR systems. Recent neutron scattering measurements [19] suggest a large, but probably finite magnetic correlation length which was argued to suggest first-order behavior. However, since our thermodynamic analysis does not require direct measurement of the correlation length, it stands correct without prior specification of the order parameter.

The extremely large value of $\alpha_{\pm} = 0.93(8)$ implies smaller exponents for the magnetization and magnetic susceptibility if the exponent identity $\alpha + 2\beta + \gamma = 2$ holds. The smaller β and γ exponents would indicate weakening of the effective magnetic coupling as T_c is approached and are likely a direct consequence of competition among charge-lattice-spin coupling. This suggests that the magnetization, alone, may not be the appropriate order parameter. However, as a cautionary point, it is noted that the thermodynamic relations impose only the inequality $\alpha + 2\beta + \gamma \geq 2$ as a restriction [20]. It is important to consider that $\alpha_{\pm} = 0.48(6)$ and $0.05(7)$ were determined for $\text{La}_{0.6}\text{Ca}_{0.4}\text{MnO}_3$ and $\text{La}_{0.75}\text{Sr}_{0.25}\text{MnO}_3$, respectively [12, 21]. Their smaller α_{\pm} values (or larger β and γ values) can be attributed to weaker charge-lattice-spin coupling as ascertained by smaller CMR effects relative to $\text{La}_{0.7}\text{Ca}_{0.3}\text{MnO}_3$ [22].

Finally, it is interesting to consider topological defect experiments. In superfluid helium, pressure is applied to move out of the superfluid state, then quickly released while measuring the defect concentration (superfluid vortex density) as a function of time [23]. Similar experiments in CMR systems could be envisioned where pressure rapidly moves the system into the *FM* state while the concentration of magnetic defects is observed versus time; such experiments are simplified by a large dT_c/dP , strong magnetic signal, and high temperatures.

In summary, a new method for investigating continuous phase transitions that uses heat capacity and thermal expansion data was presented. Its application to the *FM* phase transition of the CMR oxide $\text{La}_{0.7}\text{Ca}_{0.3}\text{MnO}_3$ has revealed an extremely large heat capacity exponent.

We thank D. Argyriou, R. Bollinger, E. Dagotto, and J. Lynn for valuable comments. Support from NSF Grant DMR-0301166 and Brazilian FAPESP Grants 99/10798-0 and 02/01856-1 is gratefully acknowledged. R.F.J. is a CNPq fellow under Grant 304647/90.

-
- [1] W. H. Zurek, Physics Reports **276**, 177 (1996).
 - [2] E. Dagotto, T. Hotta, and A. Moreo, Physics Reports **344**, 1 (2001).
 - [3] J. M. DeTeresa et al., Nature **386**, 256 (1997).
 - [4] S. W. Biernacki, Phys. Rev. B **68**, 174417 (2003).
 - [5] A. B. Pippard, *The Elements of Classical Thermodynamics* (Cambridge University Press, New York, 1957).
 - [6] Fluctuations may make the superconducting transition first order within 10^{-6} K of T_c , otherwise the transition appears second order. See: B. I. Halperin, T. C. Lubensky, and S.-K. Ma, Solid State Commun. **14**, 997 (1974).
 - [7] Some contributions to C_p are due to degrees of freedom decoupled from lattice expansion. Modeling these by $a + b'T$ near T_c , $C_p^* \equiv C_p - (a + b'T + T(\partial S/\partial T)_c)$.
 - [8] R. H. Heffner et al., Phys. Rev. Lett. **77**, 1869 (1996).
 - [9] G. M. Zhao, M. B. Hunt, and H. Keller, Phys. Rev. Lett. **78**, 955 (1997).
 - [10] J. Mira et al., Phys. Rev. B **60**, 2998 (1999).
 - [11] J. E. Gordon et al., Phys. Rev. B **65**, 024441 (2001).
 - [12] D. Kim et al., Phys. Rev. Lett. **89**, 227202 (2002).
 - [13] M. R. Lees et al., Phys. Rev. B **59**, 1298 (1999).
 - [14] Near T_c the time constant τ_2 associated with heat flow between the sample and the heat capacity platform was 100 times less than the time constant τ_1 associated with heat flow between the sample/platform and bath indicating good sample-platform thermal contact. See: J. C. Lashley et al., Cryogenics **46**, 369 (2003).
 - [15] $T_c(P)$ was fit with a second-order polynomial; the slope at $P = 0$ is 16.5(3) K/GPa.
 - [16] H. Y. Hwang et al., Phys. Rev. B **52**, 15046 (1995); J. J. Neumeier et al., *ibid.* **52**, R7006 (1995); J. M. DeTeresa et al., *ibid.* **54**, 1187 (1996); V. Laukhin et al., *ibid.* **56**, 10009 (1997).
 - [17] Without the superposition C_p^* and $7000\mu T$, successful determination of α_{\pm} alone does not establish continuous (second-order) behavior since the error allows for $\alpha_{\pm} \geq 1$. We note a mean field result where α_{\pm} can be as large as 1 for a continuous phase transition. See: D. Kim, P. M. Levy, and L. F. Uffer, Phys. Rev. B **12**, 989 (1975).
 - [18] Prepared by sintering oxide and carbonate powders (5 intermediate grindings, maximum reaction temperature of 1375°C); $T_c = 253.4$ K.
 - [19] C. P. Adams et al., Phys. Rev. B **70**, 134414 (2004).
 - [20] G.S. Rushbrooke, J. Chem. Phys. **39**, 842 (1963).
 - [21] D. Kim et al., Phys. Rev. B **65**, 214424 (2002).
 - [22] R. Mahendiran et al., Phys. Rev. B **51**, (1995) 14103.
 - [23] P. C. Hendry et al., Nature **368**, 315 (1994).